



## Scandanolone from *Cudrania tricuspidata* fruit extract suppresses the viability of breast cancer cells (MCF-7) *in vitro* and *in vivo*



Xinwei Jiang<sup>a</sup>, Chunting Cao<sup>a</sup>, Weiwei Sun<sup>a</sup>, Zisheng Chen<sup>b</sup>, Xusheng Li<sup>a</sup>, Lutfun Nahar<sup>c</sup>, Satyajit D. Sarker<sup>c</sup>, Milen I. Georgiev<sup>d</sup>, Weibin Bai<sup>a,\*</sup>

<sup>a</sup> Department of Food Science and Engineering, Institute of Food Safety and Nutrition, Guangdong Engineering Technology Center of Food Safety Molecular Rapid Detection, Jinan University, Guangzhou, PR China

<sup>b</sup> Department of Respiratory Medicine, The Sixth Affiliated Hospital of Guangzhou Medical University, Qingyuan, PR China

<sup>c</sup> Medicinal Chemistry and Natural Products Research Group, School of Pharmacy and Biomolecular Sciences, Liverpool John Moores University, James Parsons Building, Byrom Street, Liverpool, L3 3AF, England, UK

<sup>d</sup> Group of Plant Cell Biotechnology and Metabolomics, Institute of Microbiology, Bulgarian Academy of Sciences, Plovdiv, Bulgaria

### ARTICLE INFO

#### Keywords:

Polyphenols  
Flavonoid  
MCF-7 cells  
Warangalone  
Toxicity  
Xenograft model

### ABSTRACT

Scandanolone, an isoflavone, has shown anti-cancer potential. In this study, we extracted scandanolone from *Cudrania tricuspidata* fruit and evaluated its anti-breast cancer effects as well as toxicity in cell and animal models. In cell model, scandanolone suppressed the breast cancer MCF-7 cells viability, ceased mitotic cell cycle, decreased mitochondrial membrane potential, up-regulated cleaved caspase-3 and promoted the phosphorylation of p53. Additionally, this isoflavone promoted cell apoptosis and induced a sustained activation of the phosphorylation of p38 and ERK, but not JNK and Akt. The effects were further verified in a human MCF-7 breast cancer xenograft model, where scandanolone efficiently suppressed the cancer growth and increased apoptotic cells in tumor tissue. However scandanolone has also shown certain toxicity to normal hepatocytes and breast epithelial cells. It could be concluded that scandanolone suppressed the growth of breast cancer cells, but its toxicity towards normal cells might limit its potential clinical use.

### 1. Introduction

Breast cancer is the most common malignancy in women, resulting a high rate of mortality in both developed and developing countries (Ferlay et al., 2015). In the USA, the new cases of breast cancer is the first outstanding cancer on the cancer list, which takes up to 29% of all cancer types and the death rate is about 14% of all deaths from cancer (Siegel et al., 2016). The ever-growing incidence of breast cancer, creating financial burden to the society, calls for the discovery of new efficient preventative and therapeutic measures. Chemotherapeutic drugs such as paclitaxel and anthracyclines induce apoptosis and inhibit the proliferation of the cancer cells. However, some of the patients are not sensitive to these drugs, which may also lead to undesirable side effects to normal cells (Chen et al., 2017). Furthermore, some recent studies have shown that ordinary chemotherapy might enhance tumor vascularization, which further leads to resistance of tumor removal

(Zhang et al., 2016). Scientist have been continuously searching for the new ideal anticancer drugs with high efficacy, low toxicity and side effects, and phytochemicals from plant food are under active consideration (Wilsher et al., 2017).

Breast cancer appears to be closely related to the daily diet. The estrogen-related dietary pattern increases the risk of breast cancer (Gunter et al., 2018), whereas some of the polyphenol metabolites suppresses breast cancer cells proliferation (Teixeira et al., 2017). Flavonoid-enriched extracts could suppress the tumor proliferation and induce apoptosis via p53 (Vadde et al., 2016). Some flavonoids also have shown inhibition of cathepsin B in some cancer cells, which is related to the cell migration (Li et al., 2016). Moreover, flavonoid-rich extracts could also target Akt phosphorylation and inhibit angiogenesis in tumor (Zhang et al., 2018). These studies formed the basis for anticancer potential of flavonoids. Interestingly, where most of the widespread anticancer drugs have severe side effects, the reported anti-

**Abbreviations:** *C. tricuspidata*, *Cudrania tricuspidata*; MAPKs, mitogen-activated protein kinases; JNK, c-Jun NH(2)-terminal kinase; ERK, extracellular signal-regulated kinase; PARP, poly-ADP-ribose polymerase; MMP, mitochondrial membrane potential

\* Corresponding author. Department of Food Science and Engineering, Institute of Science and Technology, Jinan University, 601 Huangpu Road, Guangzhou, 510632, PR China.

E-mail address: [baiweibin@163.com](mailto:baiweibin@163.com) (W. Bai).

<https://doi.org/10.1016/j.fct.2019.02.020>

Received 18 December 2018; Received in revised form 31 January 2019; Accepted 8 February 2019

Available online 10 February 2019

0278-6915/ © 2019 Elsevier Ltd. All rights reserved.



## Cudrania tricuspidata fruit

Fig. 1. *C. tricuspidata* fruit.

cancer flavonoids, such as anthocyanidin in berry, were safe to normal cells, but only toxic to cancer cells, (Aqil et al., 2017). However, most of these flavonoids are less effective on the cancer cells suppression, and most of the anticancer studies were limited to *in vitro* cells studies with insufficient *in vivo* tests, making the evidence for anti-breast cancer potential of flavonoids refutable.

*Cudrania tricuspidata* (*C. tricuspidata*) is a deciduous tree from the family Moraceae, mainly distributed in China, Korea, Japan and Africa (Li et al., 2018). The entire *C. tricuspidata* plant has been used as a traditional medicine for curing neuritis and inflammation in some parts of Asia (Kwon et al., 2016a). Notably, the wild *C. tricuspidata* fruit is a red and edible berry (Fig. 1), which contains several bioactive compounds (Hiep et al., 2015). *C. tricuspidata* extract has been reported to possess antioxidant activity and inhibitory effects on nitric oxide synthase (Xin et al., 2017). Recent studies have shown that the bioactive compounds from *C. tricuspidata* may exert anti-cancer effect. Crude extracts of the stem of *C. tricuspidata* could induce apoptosis in SiHa cervical cancer cells (Kwon et al., 2016b). Scandanolone, an isoflavone from *C. tricuspidata* fruit, could inhibit the proliferation and migration of human melanoma cells and additionally promote cells apoptosis via autophagy flux (Hu et al., 2017). However, the individual component in *C. tricuspidata* fruit has been rarely investigated with respect to the anti-breast cancer activity.

In this study, we purified and identified efficient anti-breast cancer components from *C. tricuspidata* fruit, investigated the biological effects and the related mechanism of the most efficient compound on breast cancer MCF-7 cells. Additionally, we explored the anti-breast cancer effect of scandanolone in a human cancer xenograft model.

## 2. Materials and methods

### 2.1. Materials

Hematoxylin, eosin, loading buffer, TUNEL assay kit and CCK8 were purchased from Beyotime Biotechnology (Shanghai, China). Fetal bovine serum (FBS) was purchased from Sigma-Aldrich (St. Louis, MO, USA). Primary antibodies against pro-caspase-3, PARP, Bcl-2, Bax, Bcl-xL, Bad, p53, p-p53 were obtained from Cell Signaling Technology (Beverly, MA, USA). Anti-GAPDH, ERK, p-ERK, Akt, p-Akt, p38, p-p38, JNK, p-JNK and secondary anti-rabbit, anti-mouse antibody were purchased from Santa Cruz Biotechnology (Dallas, Texas, USA). Paclitaxel was purchased from MedChemExpress (MCE, New Jersey, USA). All the rest of the chemicals used in the study, including DMF, Tween 80 are analytically pure and supplied from Sigma-Aldrich (St. Louis, MO,

USA).

### 2.2. Scandanolone purification and identification

Frozen *C. tricuspidata* fruits were smashed and soaked in methanol (1:20 w/v) in triplicate. The extract was concentrated in a rotary evaporator, resuspended in petroleum ether, ethyl acetate or n-butyl alcohol separately. After the primary test of CCK8 on breast cancer MCF-7 cells, the most efficient ethyl acetate extract was mixed with petroleum ether and subsequently subjected to silica column chromatography. A mixture of petroleum ether and ethyl acetate with a ratio ranging from 100:3 to 0:100 was used for gradient elutions. Different fractions were collected, subsequently separated and combined by thin-layer chromatography using vanillin in sulfuric acid spray to locate the spots. The combined fractions were subjected to a Sephadex LH-20 gel column (25 mm × 1200 mm) chromatography using mobile phase comprising chloroform and methanol (1:1), the fractions were collected and recrystallized (Hu et al., 2017). The different crystals were analyzed and identified by liquid chromatography-mass spectrometry (LC-MS) and X-ray single crystal diffraction. Total Antioxidant Capacity Assay Kit with ABTS method (T-AOC) was adopted to primarily evaluate the bioactivities of the purified crystals. Briefly, antioxidants inhibited the oxidation of ABTS, which was changed to be ABTS<sup>+</sup> and detected under the wavelength of 405 nm. The antioxidative abilities of different chemicals were measured and compared with the standard curve of Trolox.

### 2.3. Cell culture

The human breast tumor line MCF-7 was used for the experiments. Cells were cultured in high glucose Dulbecco's modified Eagle's medium (DMEM, Gibco, Thermo Fisher, MA, USA) with 10% FBS and 1% penicillin/streptomycin, at 37 °C under 5% CO<sub>2</sub>. Normal liver cell line LO-2 and normal breast cell line MCF-10A were sustained in RPMI-1640 culture medium (Gibco, Thermo Fisher, MA, USA) with 10% FBS and 1% penicillin/streptomycin, at 37 °C under 5% CO<sub>2</sub>.

### 2.4. Cell viability and proliferation

The MCF-7 cells were planted in 96 well plate with a concentration of  $3 \times 10^4$ /mL, 200  $\mu$ L per well. Twelve hour later, cells were treated with scandanolone at different concentrations (5, 10, 15, 25  $\mu$ g/mL) for 12–72 h. At the end of the incubation, to each well was added 20  $\mu$ L CCK8 solution and kept in 37 °C for another 4 h. Then the plate was shaken and measured at 570 nm using a BIO-RAD Microplate Reader. Cells viability of LO-2 and MCF-10A cells were also evaluated with the treatment of scandanolone. LO-2 and MCF-10A cells with a total number of  $1 \times 10^4$ /mL per well were planted in a 96 well plate. After 12 h to let the cells adhere in the well, scandanolone or paclitaxel were used to treat the cells for another 48 h (Afrin et al., 2016). Cells morphology were studied under an inverted microscope, and subsequently CCK8 were added for the evaluation of cells viability.

### 2.5. Cell migration test

The MCF-7 cells were firstly cultured in a 6 well dish with a total number of  $5 \times 10^5$  cells per well for 12 h. Subsequently, the cells at the bottom of each well was scratched with a 200  $\mu$ L tip, and the culture dish was washed by PBS for twice to remove the loose cells. The cells were then cultured with high glucose DMEM, and treated with scandanolone or vehicle for 1 h, 24 h, and 48 h. At each time point, cells were observed under microscope of 40 × magnification, and typical pictures were taken (Jiang et al., 2017a).

## 2.6. Cell-cycle analysis

The MCF-7 cells were treated with scandanolone at 10–15  $\mu\text{M}$  for 48 h. Then, cells were harvested and fixed with ice-cold ethanol for 2 h. Cells were subsequently washed by PBS for twice and stained with propidium iodide medium, and finally examined by FACS sort flow cytometer and analyzed by FCS Express 4 software (Zafar et al., 2017).

## 2.7. Mitochondrial membrane potential detection

MCF-7 cells were planted into 6 well plates with an amount of  $4 \times 10^4$  per well and cultured for 24 h. Then cells were treated with scandanolone (5, 10, 15  $\mu\text{g}/\text{mL}$ ) for another 48 h. Thereafter, cells were harvested and subsequently incubated with JC-1 working solution for 20 min, at 37 °C. Following, cells were washed with staining buffer for once and then detected by flow cytometry, and the results were analyzed by Flowjo software (Kwon et al., 2016b).

## 2.8. Western blotting analysis

The MCF-7 cells were cultured and intervened by scandanolone as mentioned above. Western blotting was used following the previous studies (Jiang et al., 2017b), briefly as below: cells were harvested and disrupted with RIPA lysis, which was added with 1% PMSF and cocktail protease inhibitor. Subsequently, cells solutions were centrifuged at 12000 g for 15 min at 4 °C. The supernatant was collected and the protein concentration was quantified by BCA protein assay kit. Samples were mixed with loading buffer and boiled at 100 °C for 5 min. SDS-PAGE was used to separate proteins with different molecular weights, then the protein bands were transferred onto a polyvinylidene fluoride membrane (PVDF). Membranes with protein were then blocked by 5% skim milk in TBST for 1.5 h, followed by incubation with primary antibody over night at 4 °C on a rocker. Secondary antibody were then incubated with the membranes for another 1.5 h at room temperature, and the bands were incubated with ECL assay and visualized by a chemiluminescence system.

## 2.9. Animals raising

The protocol of the animal test was approved by the Animal Care and Protection Committee of Jinan University (Guangzhou, PR China). Additionally, all the animals were fed and intervened following the guidance of the Care and Use of Laboratory Animals. Female athymic nude mice (nu/nu), 5 weeks old, were purchased from Ling Chang biotechnology (Shanghai, China), and kept in a SPF environment of Animal Center of Jinan University. Mice were housed at 23–27 °C and under 40%–70% humidity, with a 12-h light/dark cycle, *ad libitum* access to water and chow. After a week of accommodation, mice were randomly divided into 4 groups, and received different treatments.

## 2.10. Human cancer xenograft models

The MCF-7 human breast tumor cells were harvested with Trypsin EDTA, washed three times with PBS and suspended at a cell density of  $1 \times 10^7$  in saline medium. Animals were anaesthetized with isoflurane and placed in a supine position. 100  $\mu\text{L}$  Tumor cells medium were slowly injected into the right axillary subcutaneous of each mouse (Khaled et al., 2016). After 12 days of establishing the animal model, succeeded subjects with a tumor of 75–80  $\text{mm}^3$  were randomly divided into three groups, 10 mice per group. Sandenolone were dissolved in a mixed vehicle of normal saline: DMF: Tween 80 = 88:10:2, and injected through the tail vein with a dose of 5  $\text{mg}/\text{kg}/\text{bw}$  or 7.5  $\text{mg}/\text{kg}/\text{bw}$ , once alternate days. The control group was received with vehicle only. Mice were intervened for 28 days and then sacrificed for further analysis.

## 2.11. Tumor growth evaluation

The tumor size was evaluated by measuring two perpendicular tumor diameters: length and width, where they represent the longer and shorter tumor diameters, respectively. Diameters were measured by a slide caliper. Tumor volumes were calculated using the formula:  $V = \text{length} \times \text{width}^2 \times 0.5$  (de Souza et al., 2014). Based on the results of tumor volume measurement, relative tumor volume (RTV) were calculated according to the following formula:  $\text{RTV} = V_t/V_0$ .  $V_0$  stands for the initial volume of tumor before intervention,  $V_t$  stands for the tumor volume during or after the treatment. Then relative tumor proliferation rate T/C (%) is gained according the following formula:  $T/C = T_{\text{RTV}}/C_{\text{RTV}} \times 100\%$ ,  $T_{\text{RTV}}$  means the relative tumor volume of the group treated with sandenolone,  $C_{\text{RTV}}$  means the relative tumor volume of control group received vehicle only. After the mice were sacrificed, tumor growth inhibition rate (IR) was adopted following the calculation:  $\text{IR} (\%) = (\text{tumor weight of control group} - \text{tumor weight of treatment group})/\text{tumor weight of control group} \times 100\%$ . Generally, the  $\text{IR} \geq 60\%$  and  $p < 0.05$  are considered as statistically significant (Khaled et al., 2016).

## 2.12. Histological analysis and immunofluorescence staining

Tumor tissues were fixed in 4% paraformaldehyde for 48 h and thereafter embedded in paraffin. The blocks were cut into 4  $\mu\text{m}$  thickness slides and stained by hematoxylin and eosin (H&E) for pathological analysis. Based on Nottingham grading system, the Nottingham Histologic Score were calculated, which is a strong and independent predictor of outcome (Elston and Ellis, 1991; Rakha et al., 2012). TUNEL staining was following the guidance of assay kit. Briefly, tissue slides were treated by proteinase K for 20 min, and washed by PBS for three times. Slides were incubated with TUNEL assay for 1 h in a dark and wet box, then stained with DAPI for 15 min. The slides were examined under fluorescence microscope using Cy3 and DAPI channel. The other immunofluorescence tests about pro-caspase-3, E-cadherin, MMP-9, Ki-67, p-p38 were operated similarly, but with the specific primary antibodies and fluorescent secondary antibodies. The fluorescence intensity was measured by Image J for the quantitative analysis. Additionally, heart, liver, kidney and spleen tissue was collected and operated same as the tumor tissue for the evaluation of toxic effects of the scandanolone treatment.

## 2.13. Statistical analysis

All the data are presented as mean  $\pm$  SEM. The significances of different groups were calculated by one-way ANOVA, and was followed by Bonferroni test for further test of the two groups. The Kruskal–Wallis rank sum test was used for the evaluation of the Nottingham histological score.  $p < 0.05$  was considered the significant difference. Graph Pad Prism 5.0 software (San Diego, CA, USA) was used for graphing and statistical analysis.

## 3. Results

### 3.1. The identification of the extracts from *C. tricuspidata* fruit and the primary test

The methanol extract of *C. tricuspidata* fruits was concentrated with a rotary evaporator, then resuspended in petroleum ether, ethyl acetate and *n*-butyl alcohol separately. Different fractions were tested for their anti-cancer ability by the CCK8 assay on MCF-7 breast cancer cells. As shown in Fig. 2, the ethyl acetate extract has shown the most significant suppression on the viability of MCF-7 cells. Subsequently, the ethyl acetate extract was purified by silica column chromatography and Sephadex LH-20 gel column, thereafter three components were obtained. The first one was identified as scandanolone by the analysis of single

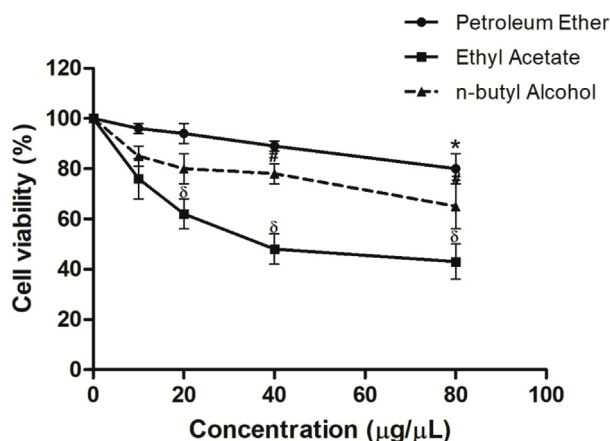


**Fig. 2.** The inhibition rate of different fractions from *C. tricuspidata* fruit on the MCF-7 cells. MCF-7 cells were cultured and treated by the DMSO dissolved different *C. tricuspidata* fruit extracts with different concentrations for 24 h, and the inhibition rate compared with control group was measured by CCK8 assay. The results were expressed as mean  $\pm$  SEM from three independent experiments ( $n = 3$ ). \* $p < 0.05$ , # $p < 0.05$ ,  $\delta p < 0.05$  significantly different compared with the relative control group.

crystal diffraction and LC-MS (Fig. 3A–C), and its purity of was higher than 97% based on HPLC measurement (Fig. 3D). The other two molecules were identified as 4'-*O*-methyl-alpinum-isoflavone and alpinum-isoflavone (Fig. S1). All three compounds were examined for their antioxidant potential. As shown in Table 1, scandanolone was the most active compound, and the antioxidative ability of which was equal to 2.76 fold of Trolox. Additionally, 1 M alpinum-isoflavone was equal

**Table 1**

The anti-oxidant capability and MCF-7 inhibition efficiency of pure compounds isolated from *C. tricuspidata* fruit extract<sup>a</sup>.

	ABTS <sup>b</sup>	MCF-7 IC <sub>50</sub> (µmol/L)
Scandanolone	2.76 $\pm$ 0.52	38.5 $\pm$ 2.3
Alpinum-isoflavone	0.64 $\pm$ 0.25	76.2 $\pm$ 4.1
4'- <i>O</i> -Methyl-alpinum-isoflavone	< 0.025	> 200.0

<sup>a</sup> Values are expressed as mean  $\pm$  SEM.

<sup>b</sup> The relative reactive oxygen species scavenging capability compared with Trolox.

to 0.64 M Trolox, but 4'-*O*-Methyl-alpinum-isoflavone showed weak antioxidant activity. All three compounds were then evaluated for the anti-breast cancer potential in MCF-7 cells. After 24 h of incubation, scandanolone showed the best inhibition of the viability of the cells, and the IC<sub>50</sub> was 38.5 µmol/L. As a comparison, the IC<sub>50</sub> for alpinum-isoflavone was 76.2 µmol/L, and that for 4'-*O*-methyl-alpinum-isoflavone was higher than 200 µmol/L. Thus, scandanolone was the compound of interest in *C. tricuspidata* fruit for favorable anti-breast cancer effect, it was subsequently prepared from the ethyl acetate crude extract for the further studies.

### 3.2. Scandanolone inhibited the growth of breast cancer cell line MCF-7

The inhibitory effect of scandanolone was further investigated based on the dose and time dependent test. As shown in Fig. 4A, MCF-7 cells viability decreased dramatically after the incubation of scandanolone for 12–72 h. Above the dose of 5 µg/mL, scandanolone inhibited the cell viability in a dose-dependent manner, the effects magnified with longer time of incubation. Scandanolone at the concentration of 17.5 and

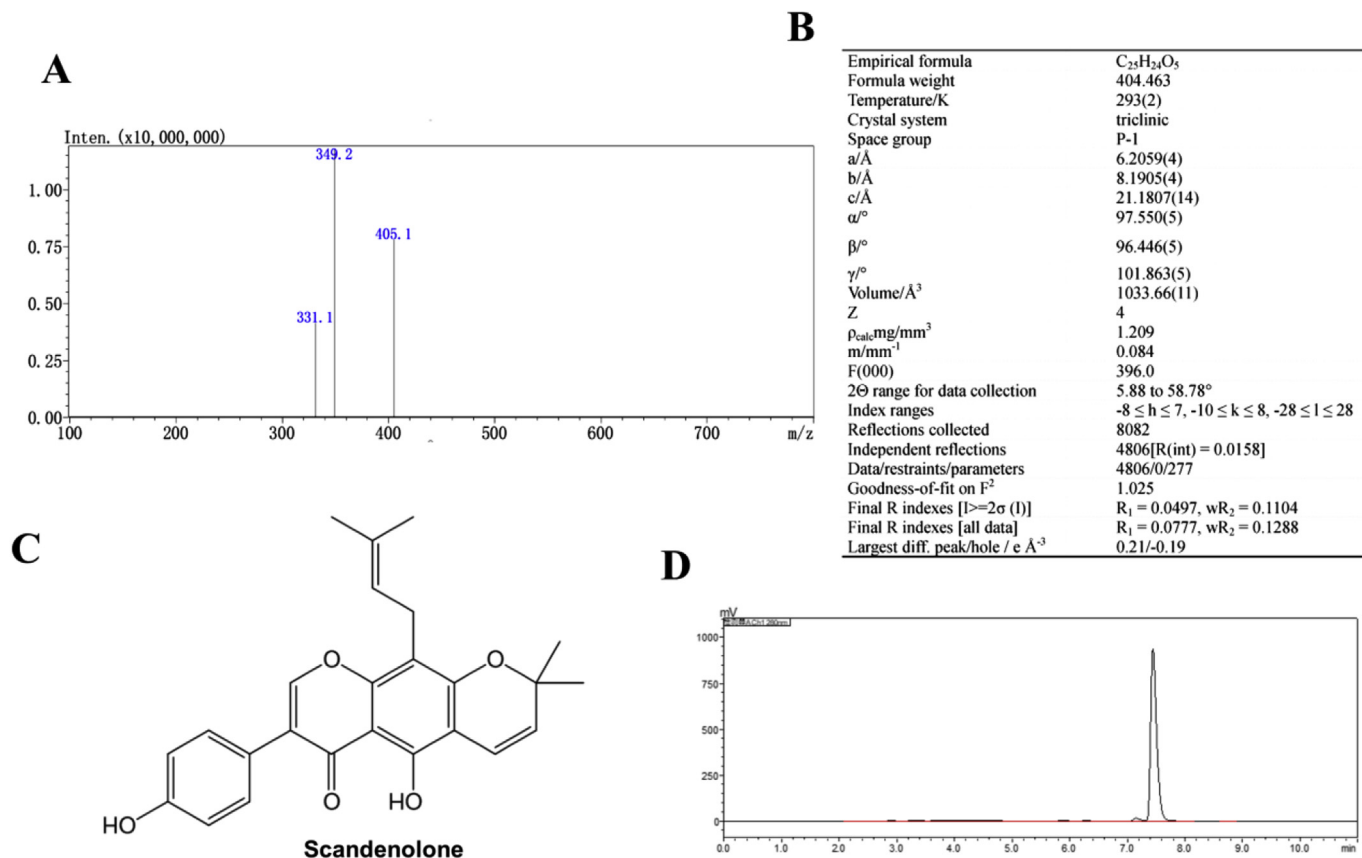


**Fig. 3.** Identification of the main compound extracted from *C. tricuspidata* fruit. (A) The secondary mass spectrometry of the substance. (B) Single crystal diffraction of the extracted compound was confirmed as scandanolone, and the (C) chemical structure of scandanolone. (D) The purity of scandanolone was measured by HPLC.

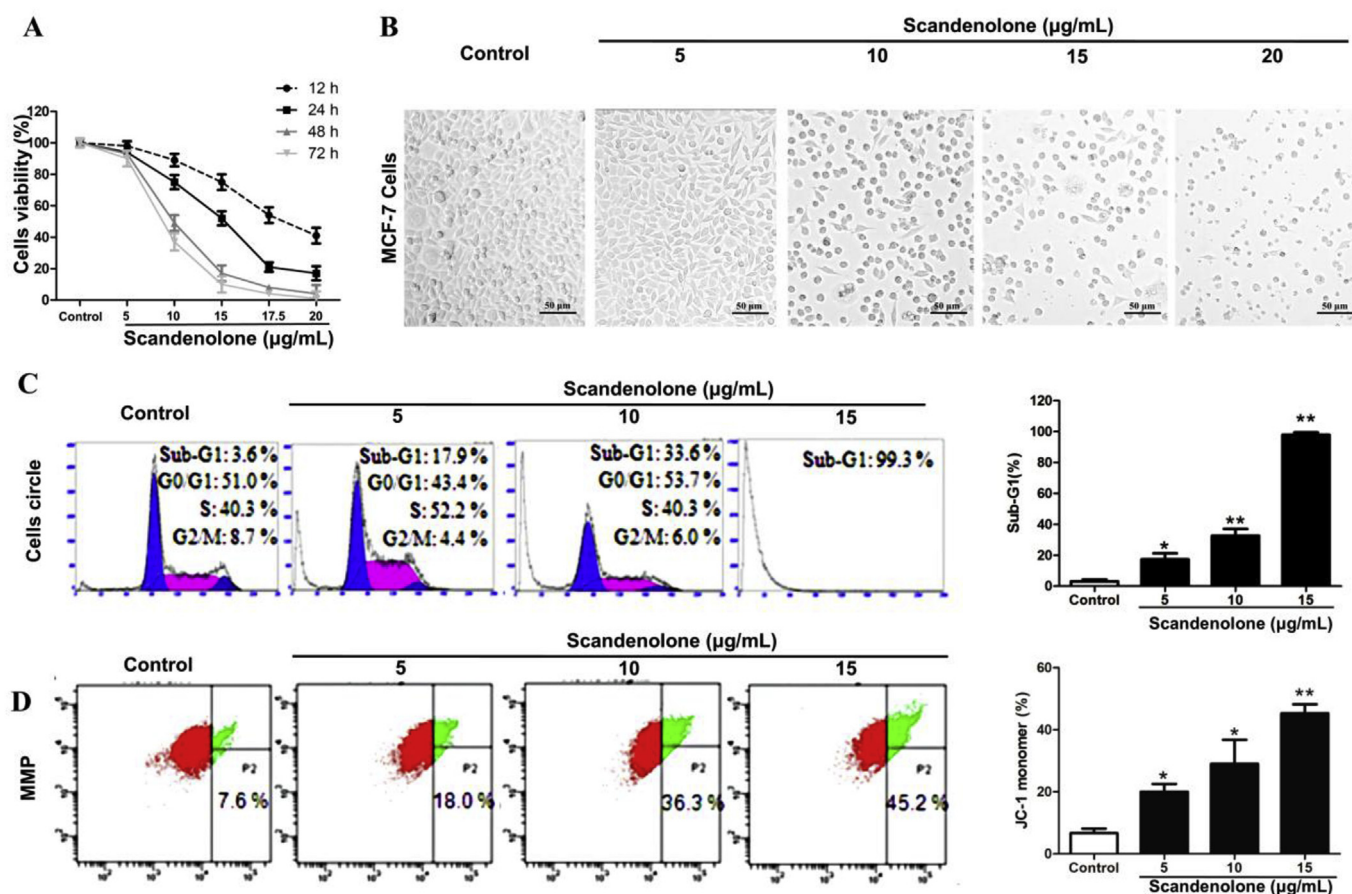


**Fig. 4.** Scandanolone inhibited the proliferation of MCF-7 cells and induced the cells apoptosis. (A) Breast cancer MCF-7 cells were incubated with scandanolone for 12–72 h, the cells viability were tested by CCK8 assay. (B) Cells were cultured 48 h and typical views of cells morphology are shown (100 × ). (C) Cell cycle distribution was examined by flow cytometry and Sub-G1 ratio was calculated. (D) Mitochondrial membrane potential was detected by fluorescence probe JC-1 and green fluorescence ratio which indicated the mitochondrial membrane damage was shown. (For interpretation of the references to colour in this figure legend, the reader is referred to the Web version of this article.)

20 µg/mL treated the MCF-7 cells for longer than 48 h, led to extreme low survival rate (8% and 4% separately). According to the morphology examination under microscope (Fig. 4B), scandanolone suppressed the cell growth, weakened the cell adherence, and caused much vesicle in cytoplasm. With higher dose of scandanolone, most of the cells shape changed, disintegrated and generated massive cell debris.

MCF-7 cells were incubated with different concentration of scandanolone for 48 h, and cell cycle was detected by flow cytometry. As shown in Fig. 4C, scandanolone significantly increased Sub-G1 ratio in a dose-dependent manner, and above 99% of cells were in the Sub-G1 phase when the treatment reached the concentration of 15 µg/mL. However, the G0/G1, S, and G2/M phases were not changed much by scandanolone. The results implicated that the treatment of scandanolone stimulated the cells into the process of apoptosis.

Mitochondrial membrane potential (MMP) indicated the capability of oxidative phosphorylation and generate ATP to sustain the regular function of mitochondrial. The damage of mitochondrial membrane potential happened in the infancy of cells apoptosis which could be detected by JC-1. As shown in Fig. 4D, normal MCF-7 cells kept high level of red fluorescence, which indicated the high integrity of mitochondrial membrane, however scandanolone treatment caused the increase of green fluorescence ratio with a dose-dependent manner, which revealed the increase of JC-1 monomer and cells apoptosis.

### 3.3. Scandanolone induced the MCF-7 cells apoptosis and suppressed the cells migration

Whole cell lysis was further evaluated for cell apoptosis by western blot (Fig. 5A), scandanolone activated pro-caspase-3 and reduced the level of PARP. Bcl-2 family mainly adheres to mitochondrial and endoplasmic reticulum, which adjust cell apoptosis. Notably, scandanolone showed no significant effect on Bcl-xL, and Bad levels, and slightly increased Bcl-2, Bax level, but the Bax/Bcl-2 level was not changed (Fig. 5B).

Furthermore, the effect of scandanolone on cells migration was examined. After the MCF-7 cells planted and scratched with a tip, cells were treated either with vehicle or 5 µg/mL scandanolone for 1 h, 24 h and 48 h. As shown in Fig. 5C, scandanolone suppressed the migration of MCF-7 cells after 24 h treatment, which indicated the suppression on the MCF-7 cells invasion.

### 3.4. Scandanolone mediated p53 and MAPKs pathway

Many of the cancers are associated with the mutation of mitogen-activated protein kinases (MAPKs). MAPKs are serine-threonine kinases that mediate various intracellular signaling including cell proliferation, differentiation and apoptosis. In our study, MCF-7 cells were treated with scandanolone at different concentrations for 24 h, afterwards the cell lysate was collected and analyzed by immunoblotting. The treatment of scandanolone induced the phosphorylation of p53, but there was no influence on total p53 level (Fig. 6). Scandanolone remarkably

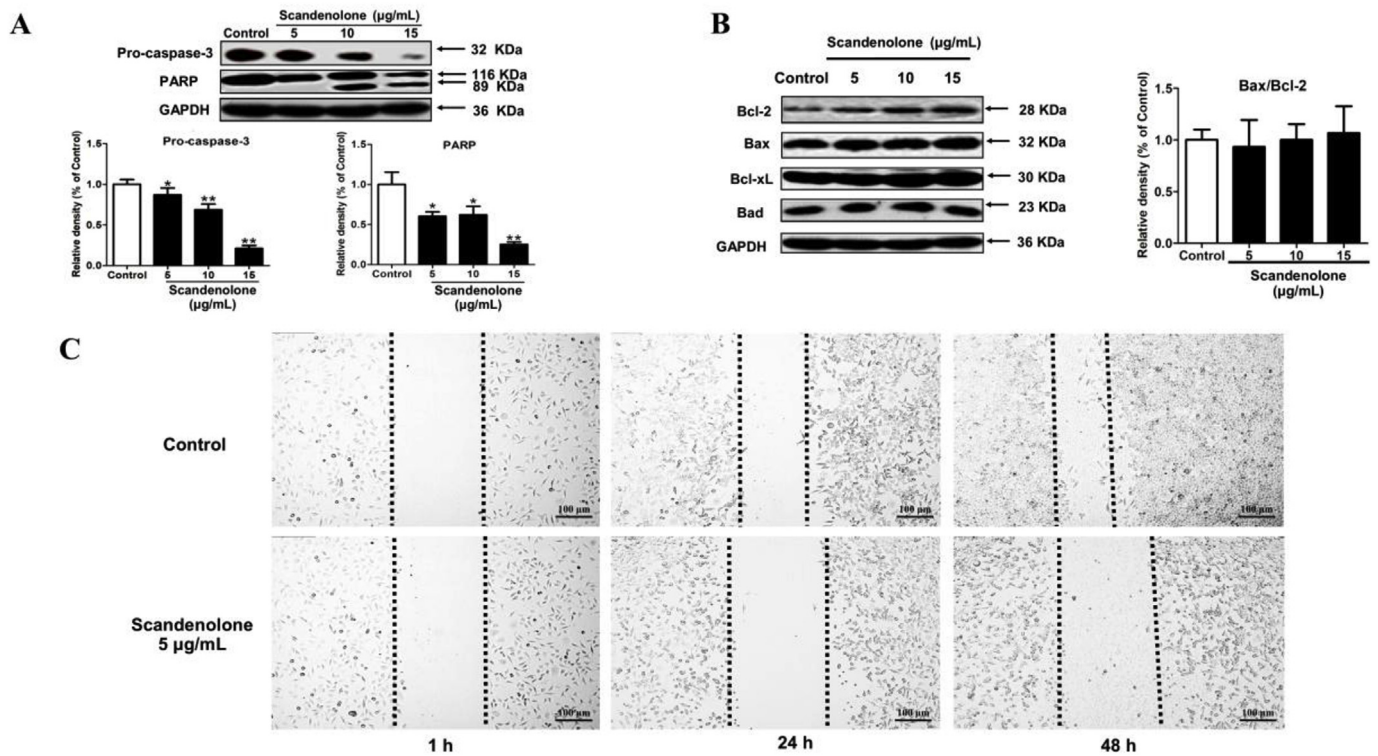


**Fig. 5.** Scandanolone inhibited apoptosis related protein expression and inhibited the cells migration. (A and B) MCF-7 cells were treated with scandanolone for 24 h, apoptotic proteins were detected by western blot. (C) Cells wound was made and treated with scandanolone for 1–48 h, then the cells migration capability was evaluated (40 ×). All data are presented as the mean ± SEM from three independent experiments (n = 3). \*p < 0.05 \*\*p < 0.01 significantly different compared with the control group.

increased the level of p-p38 and p-ERK in a dose-dependent manner. In addition, scandanolone slightly upregulated the level of p-JNK and showed no effect on p-Akt. Total p38, AKT and JNK were not changed significantly by the treatment with scandanolone.

### 3.5. Scandanolone inhibited breast tumor xenografts growth

Human breast cancer xenografts were generated by subcutaneously transplanting of MCF-7 cells into the nude mice. The initial weights of

the mice in different groups were indistinctive before intervention. After the treatment, as is shown in Fig. 7A, body weights of the mice in the vehicle group were kept increasing in the following days. However, in scandanolone treated groups, the body weights did not shift significantly. The body weight change was mainly due to the growing tumor volume. Tumor volume were kept enlarging, but scandanolone treatment of both dose repressed the tumor growth (Fig. 7B). At the end of tumor intervention, mice were anaesthetized and the volume of xenografts were much smaller in the scandanolone treated group

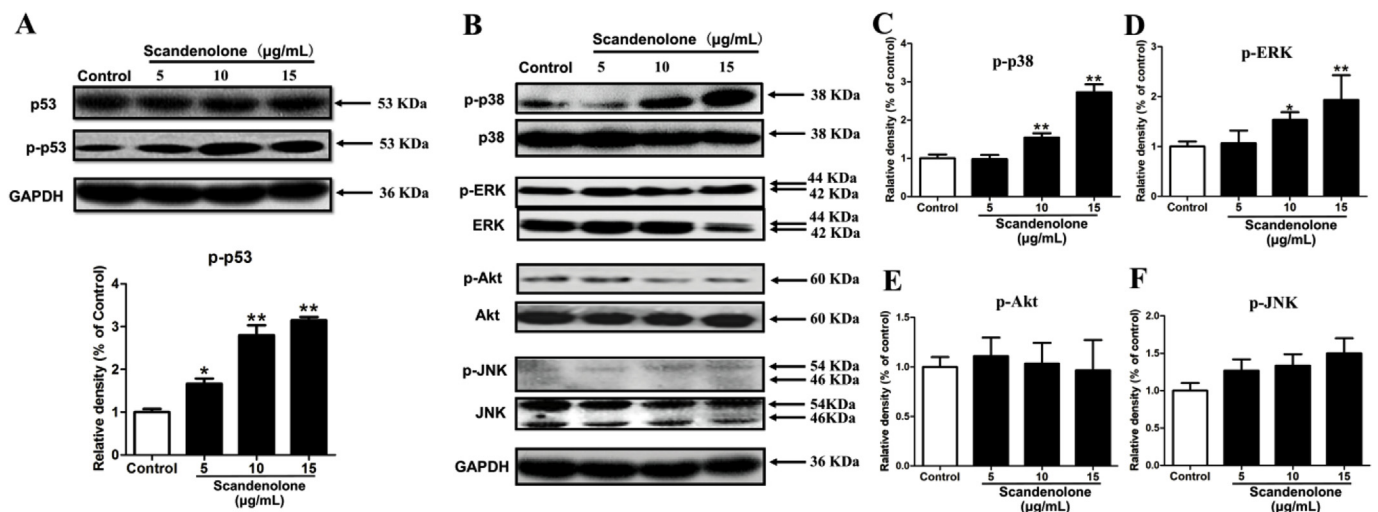


**Fig. 6.** Evaluation of scandanolone on the MAPKs signaling transduction pathway. MCF-7 cells were treated with scandanolone for 24 h, and the target proteins were measured by western blot. (A) Measurement of the protein expression p53 and (B–F) MAPKs including p-p38, p-ERK, p-Akt and JNK, which were detected and analyzed the density of gray bands by Quality One. All data are presented as the mean ± SEM from three independent experiments (n = 3). \*p < 0.05 \*\*p < 0.01 significantly different compared with the control group.

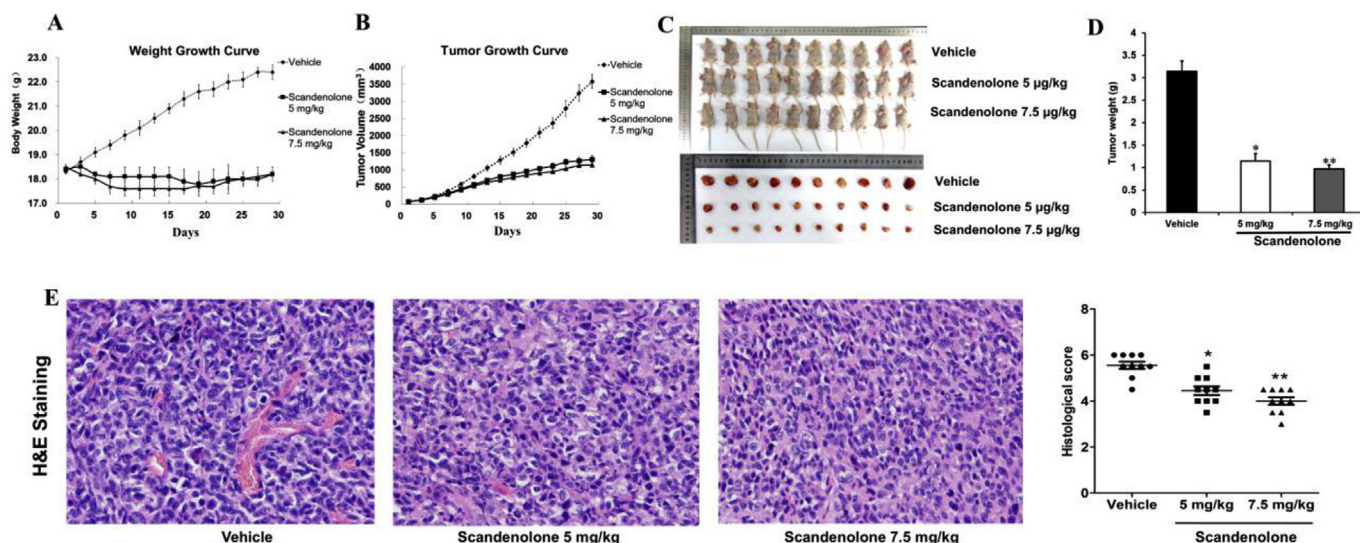


**Fig. 7.** Scandanolone inhibited the cancer tumor growth on the human breast cancer xenografts model. Mice models were established by the injection of MCF-7 cells to the right axillary subcutaneous and treated by scandanolone for 28 days. (A) Body weights were recorded, (B) tumor volume were measured by vernier caliper. (C) After mice were sacrificed, tumor tissues were separated carefully and (D) weighted. (E) Tumor tissue were fixed and cut into 4  $\mu\text{m}$  slides, H&E staining were carried out for histological analysis (200  $\times$ ) and the Nottingham Histologic Score was calculated. The results were expressed as mean  $\pm$  SEM, \* $p < 0.05$ , \*\* $p < 0.01$  compared with vehicle group.  $n = 10$ .

**Table 2**

Tumor growth parameters of scandanolone treatment on the breast cancer xenografts model.

	Animal weight		Tumor volume		Tumor weight (g)	Relative tumor proliferation rate (T/C)	Inhibition rate (IR)
	Initial (g)	Sacrificed (g)	Initial ( $\text{cm}^3$ )	Sacrificed ( $\text{cm}^3$ )			
Vehicle	18.3 $\pm$ 0.1	22.4 $\pm$ 0.3	0.08 $\pm$ 0.01	3.58 $\pm$ 0.20	3.14 $\pm$ 0.23	100%	0%
Scandanolone 5 mg/kg	18.4 $\pm$ 0.1	18.2 $\pm$ 0.1*	0.08 $\pm$ 0.01	1.31 $\pm$ 0.12**	1.15 $\pm$ 0.16**	37.11%	63.5%
Scandanolone 7.5 mg/kg	18.5 $\pm$ 0.1	18.2 $\pm$ 0.3**	0.08 $\pm$ 0.01	1.15 $\pm$ 0.07**	0.97 $\pm$ 0.09**	33.47%	69.1%

\* $p < 0.05$ , \*\* $p < 0.01$  compared with the vehicle group with significant differences.

(Fig. 7C). Both of the scandanolone treated group showed lighter tumor weight compared with vehicle group (Fig. 7D). Additionally, 7.5  $\mu\text{g}/\text{kg}$  of scandanolone treatment was more efficient than 5  $\mu\text{g}/\text{kg}$ , although showed no significance. As shown in Table 2, scandanolone treatment showed lower relative tumor proliferation rate, and both doses of scandanolone treatment led to significant inhibition rate (63.5% and 69.1% separately).

Tumor tissue slides were stained with hematoxylin and eosin stain (H&E), and viewed under a microscope with the magnifying power of 200  $\times$  (Fig. 7E). Under the treatment of scandanolone of 5 mg/kg, tumor cells still showed activated growing condition, but blood vessel and fibrosis significantly reduced compared to control group. Additionally, less infiltrating inflammatory cells were found. With a higher dose of scandanolone (7.5 mg/kg) treatment, the growing condition of tumor cells were significantly suppressed. Local tumor cells necrosis increased, blood vessels fibrosis significantly reduced compared with scandanolone 5 mg/kg group. Additionally, no inflammatory cells were detected. All the histological analysis were carried on by senior pathologists, and pathological score were calculated. Both of scandanolone treated group reduced the pathological score, which indicated the less malignant tumor growth.

### 3.6. Scandanolone induced cancer tissue cells apoptosis

Apoptosis in the tumor tissue were examined by the TUNEL assay (Fig. 8A). More apoptotic cells were shown in scandanolone treated group compared with control group, and higher dose of treatment

caused more severe cells apoptosis. Similarly, we measured the level of pro-caspase 3 (Fig. 8B) and found a significant decrease after the treatment of scandanolone, which eventually indicated the activation of caspase cascade and the cells apoptosis. Additionally, we evaluated the condition of cell invasion and proliferation. E-cadherin downregulation decreased the strength of cellular adhesion within a tissue, resulting in an increase of cellular dedifferentiation and invasiveness. This in turn might allow cancer cells to cross the basement membrane and invade surrounding tissues. As shown in Fig. 2S, the level of E-cadherin showed a slight increase after the treatment of scandanolone, which showed an alleviation of tumor aggressive condition. The level of MMP-9, Ki-67 and p-P38 did not changed much, which indicated the cells proliferation might not be influenced by the treatment of scandanolone.

### 3.7. Scandanolone showed toxicity to normal hepatocytes and breast epithelial cells

Since scandanolone inhibited the proliferation of MCF-7 cells and caused apoptosis, it was important to examine its toxicity to normal cells. Normal hepatocyte cell lines LO-2 and normal mammary epithelial cell MCF-10A were then tested. As shown in Fig. 9A and B, after the cells were treated with scandanolone for 48 h, cells viability significantly decreased when the drug dose was higher than 12.5  $\mu\text{g}/\text{mL}$ . Additionally, the toxicity of scandanolone and paclitaxel on normal cells was compared. Reassuringly, at the same concentration, scandanolone was much less toxic to cells compared with paclitaxel (Fig. 9C and D). Meanwhile, the damage of scandanolone treatment on the

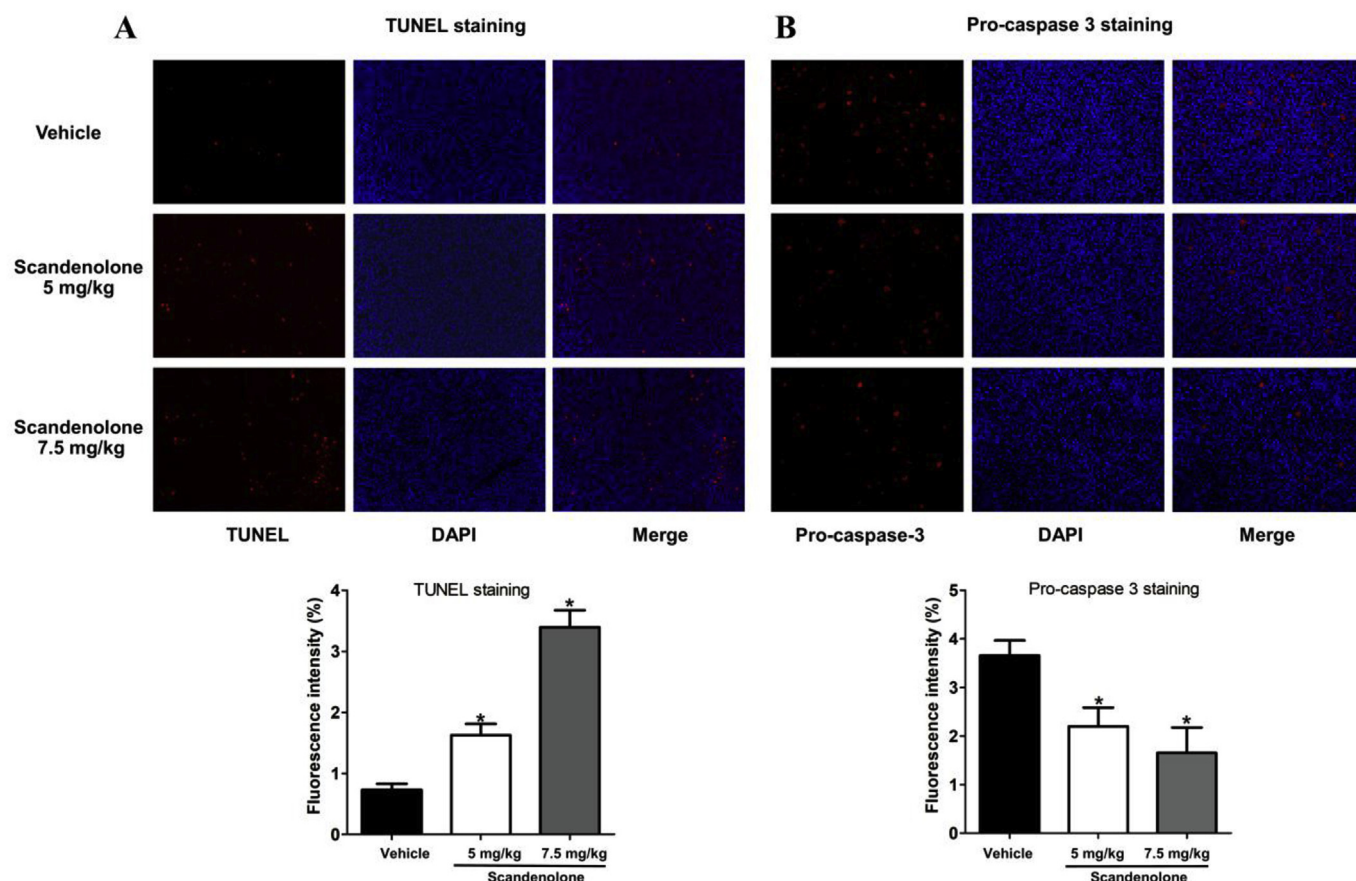


**Fig. 8.** Tumor tissue slides were performed with immunofluorescence staining. TUNEL (A), pro-caspase 3 (B) were carried for the detection of apoptotic cells, DAPI were used to mark the cell nucleus. The fluorescence was captured by a fluorescence inversion microscope system. Five random fields of the tissue slides were captured and typical pictures were shown in this figure. The fluorescence intensity was measured by Image J.  $n = 4$ ,  $200\times$ .

normal organs in the mice model was also examined. According to the histological analysis, scandenolone at the dose of 7.5 mg/kg has shown no obvious damage to heart, kidney and spleen, but obvious hepatocytes damage were detected in liver tissue (Fig. 9E).

#### 4. Discussion

Breast cancer is the major cause of cancer-related mortality in women worldwide. Scandenolone from *C. tricuspidata* fruit showed extraordinary anticancer effects, and the  $IC_{50}$  was less than  $12.5\ \mu\text{g}/\text{mL}$ , whereas some of the other flavonoids might reach to  $1000\text{--}5000\ \mu\text{g}/\text{mL}$  (Giampieri et al., 2018; Lu et al., 2018). Cancer cell apoptosis is a main target for the therapy. Apoptotic cells can be processed through the extrinsic or the intrinsic signaling pathways. The extrinsic pathway is activated at the cell surface when a specific ligand binds to its corresponding cell surface death receptor (Zhao et al., 2012). The apoptosis programs start off and sequentially activates caspase-8 and -3, which cleaves target proteins that leading to apoptosis (Ashkenazi and Dixit, 1998). In our study, scandenolone caused MCF-7 cells apoptosis and a decrease of pro-caspase-3, which indicated that the caspase-3 was activated and cleaved into subunits. Apoptosis triggered protein PARP, and the increasing of cleaved PARP was shown after the incubation of scandenolone. We also investigated the intrinsic apoptosis signaling pathways. Intrinsic death activates the mitochondrial pathway by inducing release of cytochrome *c* and formation of the apoptosome. This death pathway is mainly controlled by the proapoptotic proteins including Bax, Bak and Bid, and anti-apoptotic proteins Bcl-2, Bcl-xL (Beesoo et al., 2014). In our study, the integrity of mitochondrial membrane was destroyed by the treatment of scandenolone, but anti-

apoptotic protein Bcl-2 and Bcl-xL was not decreased, meanwhile the level of pro-apoptotic protein Bax and Bad was not increased. Therefore, scandenolone mainly mediated cell apoptosis through extrinsic apoptosis signaling pathway, not the intrinsic pathways.

Many studies have shown that MAPK signaling pathways involving JNK, p38 and ERK mediates cells apoptosis (Ravindran et al., 2011). Upon activation, p38 proteins can translocate from the cytosol to the nucleus where it orchestrates cellular responses through mediating phosphorylation of its downstream transcription factors such as caspase family (Sui et al., 2014). It is estimated that p38 may regulate mitochondrial function, thereafter cause the release of cytochrome *c* and activate caspases (Park et al., 2011). The protein p53 plays a critical role of modulating transformation, cell growth, DNA synthesis and repair, differentiation and apoptosis (Woods and Vousden, 2001). As a transcription factor, p53 targets multiple elements involved in the apoptotic pathway, including p53-regulated apoptosis-inducing protein 1 (p53AIP1) and pro-apoptotic Bcl-2 family members (Chipuk et al., 2004). Additionally, p53 is upregulated by the phosphorylation of p38 MAPK (Dewanjee et al., 2017), elevated p53 is related to the mediation of apoptosis (Zheng et al., 2018). The activated JNK can regulate a variety of transcription factors and mitochondrial proteins like Bcl-2 and Bcl-xL (Radogna et al., 2015). Our data has shown that scandenolone did not affect the level of p-JNK, and thus Bcl-2 and Bcl-xL was neither changed. Endoplasmic reticulum (ER) is essential to cellular homeostasis, strong ER stress induces apoptosis. Some stress responses require p38 MAPK but not ERK1/2 and others both p38 MAPK and ERK (Hamamura et al., 2009). In our study, p38 and ERK were both activated by the treatment with scandenolone, which indicated the activation of ER stress mediated cell apoptosis. These results were

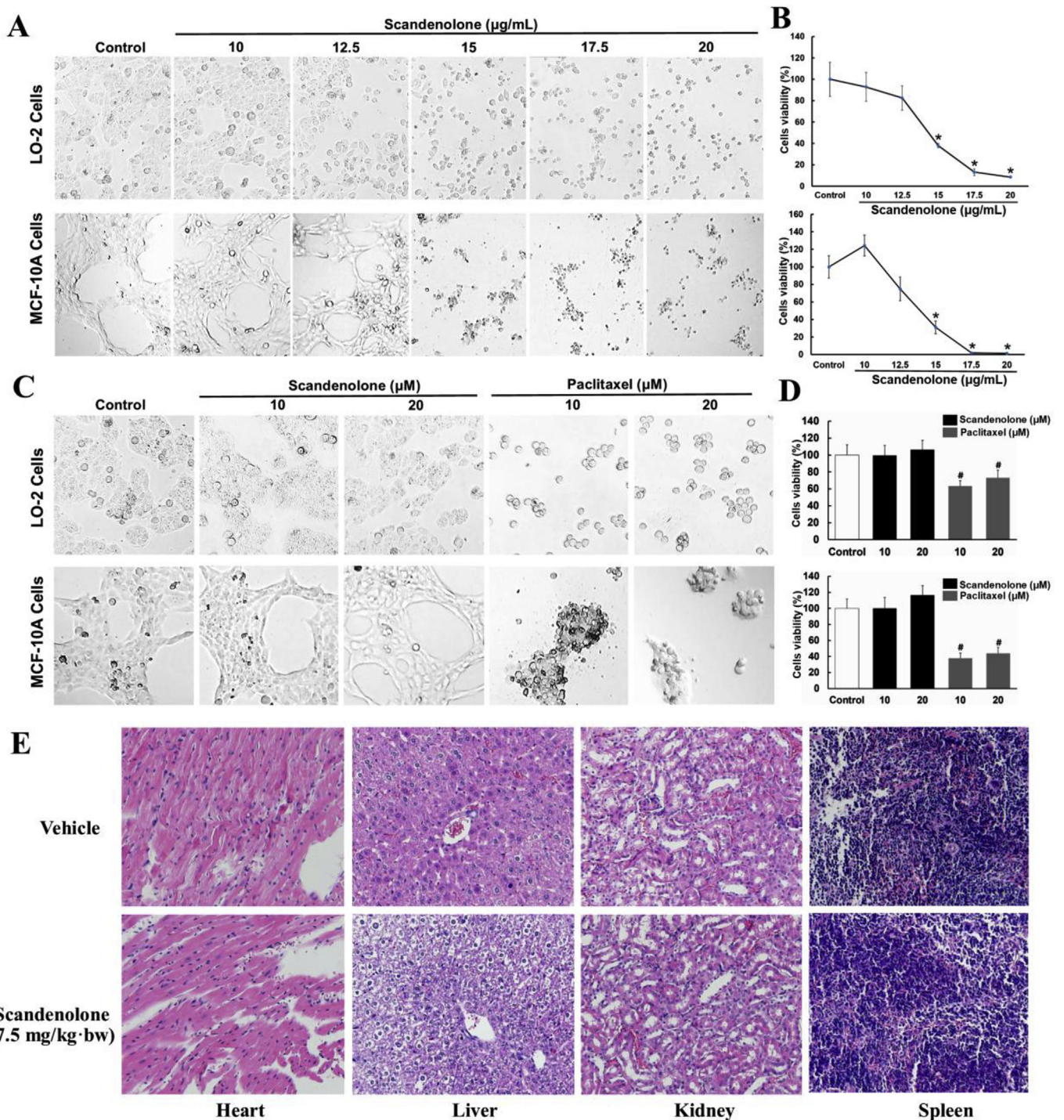


**Fig. 9.** Toxicity evaluation of scandenolone on normal cells and organs. Normal cells line LO-2 and MCF-10A were cultured for 48 h, (A) cells morphology (100 ×) and (B) cells viability were detected. (C–D) LO-2 and MCF-10A cells were cultured and treated for 48 h, and the toxicity of scandenolone and paclitaxel was compared (400 ×). (E) In animal models, histological analysis of heart, liver, kidney and spleen in vehicle and scandenolone (7.5 mg/kg) group, typical pictures were chosen in five random view fields, 200 ×. Results were expressed as mean mean ± SEM, \**p* < 0.05 compared with the control group, #*p* < 0.05 compared with the scandenolone group.

consistent with the previous studies that upregulated p38 MAPK and p-ERK in cancer cells would induce cell apoptosis (Cao et al., 2010; Deng et al., 2010).

*C. tricuspidata* is a valuable resource of bioactive compounds to protect against some chronic diseases. Extract from *C. tricuspidata* leaves were proven to prevent ethanol induced and db/db obesity mice liver injury (Kim et al., 2015; You et al., 2017). *C. tricuspidata* root extracts also protected drugs induced HepG2 damage (An et al., 2006;

Tian et al., 2005). However, our study firstly revealed that scandenolone was toxic to normal hepatocytes and breast epithelial cells. To our knowledge most of the efficient natural compounds are not specific target to cancer cells, but can induce cells apoptosis, oncosis, DNA binding, antimetosis, mediate ATP-binding cassette transporters, MAPK, p53, NF-κB, tubulin polymerization inhibition or some other pathways, which mostly exist in normal cells as well (Paier et al., 2018; Tewari et al., 2019). The compounds with lower toxicity usually have shown

less efficiency of curing cancer, whereas the efficient ones may also show high toxicity to the normal cells. Firstly, to screen the natural compounds with higher efficiency for the cancer cells meanwhile less toxicity to the normal cells. However, it is difficult to find an ideal compound, thus some of the following solutions are needed. Appropriate dosage should be chosen for a suitable therapy effect and mild side effects. Additionally, the chemical structure of the natural compounds could be chemically modified for a better bioactivity. Docetaxel and cabazitaxel are the derivatives of paclitaxel, which have shown much better inhibition of cancer cells but less side effects (Galsky et al., 2010; Lyseng-Williamson and Fenton, 2005). Last but not least, drug combination has a bright future. The combination using of the drugs may have more efficient and broader application in cancer treatment, meanwhile reduce the toxicity. Curcumin could enhance the chemotherapy effect meanwhile reverse the drug resistance (Mehta et al., 2014), which indicated a bright future for the drugs combination using on cancer therapy.

## 5. Conclusions

In summary, scandenolone, purified from *C. tricuspidata* fruit exerted strong anti-breast cancer effect. Scandenolone decreased the cell viability of breast cancer cells MCF-7, and induced p53 and MAPKs mediated cells apoptosis. In addition, scandenolone efficiently suppressed breast tumor growth in human cancer xenograft model. However, an attention should be paid to the latent toxicity of scandenolone on the normal cells. For a better development of scandenolone for clinical purposes, further studies on detoxification of scandenolone are essentially needed.

## Conflicts of interest

The authors declare no conflict of interest.

## Acknowledgements

This work was supported by the National Natural Science Foundation of China (NSFC, No. 31771983 and No. 31471588). The authors also thank the Science and Technology Program of Guangzhou (No. 201704020050).

## Appendix A. Supplementary data

Supplementary data to this article can be found online at <https://doi.org/10.1016/j.fct.2019.02.020>.

## References

- Afrin, S., Giampieri, F., Gasparrini, M., Forbes-Hernandez, T.Y., Varela-Lopez, A., Quiles, J.L., Mezzetti, B., Battino, M., 2016. Chemopreventive and therapeutic effects of edible berries: a focus on colon cancer prevention and treatment. *Molecules* 21.
- An, R.B., Sohn, D.H., Kim, Y.C., 2006. Hepatoprotective compounds of the roots of *Cudrania tricuspidata* on tacrine-induced cytotoxicity in Hep G2 cells. *Biol. Pharm. Bull.* 29, 838–840.
- Aqil, F., Jeyabalan, J., Agrawal, A.K., Kyakulaga, A.H., Munagala, R., Parker, L., Gupta, R.C., 2017. Exosomal delivery of berry anthocyanidins for the management of ovarian cancer. *Food Funct.* 8, 4100–4107.
- Ashkenazi, A., Dixit, V.M., 1998. Death receptors: signaling and modulation. *Science* 281, 1305.
- Beesoo, R., Neerghen-Bhujun, V., Bhagooli, R., Bahorun, T., 2014. Apoptosis inducing lead compounds isolated from marine organisms of potential relevance in cancer treatment. *Mutat. Res. Fund. Mol. Mech. Mutagen.* 768, 84–97.
- Cao, X.H., Wang, A.H., Wang, C.L., Mao, D.Z., Lu, M.F., Cui, Y.Q., Jiao, R.Z., 2010. Surfactin induces apoptosis in human breast cancer MCF-7 cells through a ROS/JNK-mediated mitochondrial/caspase pathway. *Chem. Biol. Interact.* 183, 357–362.
- Chen, X.X., Lam, K.H., Chen, Q.X., Leung, G.P.H., Tang, S.C.W., Sze, S.C.W., Xiao, J.B., Feng, F., Wang, Y., Zhang, K.Y.B., Zhang, Z.J., 2017. Ficus virens proanthocyanidins induced apoptosis in breast cancer cells concomitantly ameliorated 5-fluorouracil induced intestinal mucositis in rats. *Food Chem. Toxicol.* 110, 49–61.
- Chipuk, J.E., Kuwana, T., Bouchier-Hayes, L., Droin, N.M., Newmeyer, D.D., Schuler, M., Green, D.R., 2004. Direct activation of Bax by p53 mediates mitochondrial membrane permeabilization and apoptosis. *Science* 303, 1010–1014.
- de Souza, C.M., Araújo e Silva, A.C., de Jesus Ferracioli, C., Moreira, G.V., Campos, L.C., dos Reis, D.C., Lopes, M.T.P., Ferreira, M.A.N.D., Andrade, S.P., Cassali, G.D., 2014. Combination therapy with carboplatin and thalidomide suppresses tumor growth and metastasis in 4T1 murine breast cancer model. *Biomed. Pharmacother.* 68, 51–57.
- Deng, Y.T., Huang, H.C., Lin, J.K., 2010. Rotenone induces apoptosis in MCF-7 human breast cancer cell-mediated ROS through JNK and p38 signaling. *Mol. Carcinog.* 49, 141–151.
- Dewanjee, S., Joardar, S., Bhattacharjee, N., Dua, T.K., Das, S., Kalita, J., Manna, P., 2017. Edible leaf extract of *Ipomoea aquatica* Forssk. (Convolvulaceae) attenuates doxorubicin-induced liver injury via inhibiting oxidative impairment, MAPK activation and intrinsic pathway of apoptosis. *Food Chem. Toxicol.* 105, 322–336.
- Elston, C.W., Ellis, I.O., 1991. Pathological prognostic factors in breast cancer. I. The value of histological grade in breast cancer: experience from a large study with long-term follow-up. *Histopathology* 19, 403–410.
- Ferlay, J., Soerjomataram, I., Dikshit, R., Eser, S., Mathers, C., Rebelo, M., Parkin, D.M., Forman, D., Bray, F., 2015. Cancer incidence and mortality worldwide: sources, methods and major patterns in GLOBOCAN 2012. *Int. J. Cancer* 136, E359–E386.
- Galsky, M.D., Dritselis, A., Kirkpatrick, P., Oh, W.K., 2010. Cabazitaxel. *Nature reviews. Drug Discov.* 9, 677–678.
- Giampieri, F., Gasparrini, M., Forbes-Hernandez, T.Y., Mazzoni, L., Capocasa, F., Sabbadini, S., Alvarez-Suarez, J.M., Afrin, S., Rosati, C., Pandolfini, T., Molesini, B., Sanchez-Sevilla, J.F., Amaya, I., Mezzetti, B., Battino, M., 2018. Overexpression of the anthocyanidin synthase gene in strawberry enhances antioxidant capacity and cytotoxic effects on human hepatic cancer cells. *J. Agric. Food Chem.* 66, 581–592.
- Günter, M.A., McLain, A.C., Merchant, A.T., Sandler, D.P., Steck, S.E., 2018. A dietary pattern based on estrogen metabolism is associated with breast cancer risk in a prospective cohort of postmenopausal women. *Int. J. Cancer* 143, 580–590.
- Hamamura, K., Goldring, M.B., Yokota, H., 2009. Involvement of p38 MAPK in regulation of MMP13 mRNA in chondrocytes in response to surviving stress to endoplasmic reticulum. *Arch. Oral Biol.* 54, 279–286.
- Hiep, N.T., Kwon, J., Kim, D.-W., Hwang, B.Y., Lee, H.-J., Mar, W., Lee, D., 2015. Isoflavones with neuroprotective activities from fruits of *Cudrania tricuspidata*. *Phytochemistry* 111, 141–148.
- Hu, Y., Li, Z., Wang, L., Deng, L., Sun, J., Jiang, X., Zhang, Y., Tian, L., Wang, Y., Bai, W., 2017. Scandenolone, a natural isoflavone derivative from *Cudrania tricuspidata* fruit, targets EGFR to induce apoptosis and block autophagy flux in human melanoma cells. *J. Funct. Foods* 37, 229–240.
- Jiang, X., Shen, T., Tang, X., Yang, W., Guo, H., Ling, W., 2017. Cyanidin-3-O-beta-glucoside combined with its metabolite protocatechuic acid attenuated the activation of mice hepatic stellate cells. *Food Funct.* 8, 2945–2957.
- Khaled, M., Belaoui, G., Jiang, Z.-Z., Zhu, X., Zhang, L.-Y., 2016. Antitumor effect of Deoxydopoyllotoxin on human breast cancer xenograft transplanted in BALB/c nude mice model. *J. Infect. Chemother.* 22, 692–696.
- Kim, O.K., Nam, D.E., Jun, W., Lee, J., 2015. *Cudrania tricuspidata* water extract improved obesity-induced hepatic insulin resistance in db/db mice by suppressing ER stress and inflammation. *Food Nutr. Res.* 59, 29165.
- Kwon, J., Hiep, N.T., Kim, D.-W., Hong, S., Guo, Y., Hwang, B.Y., Lee, H.J., Mar, W., Lee, D., 2016a. Chemical constituents isolated from the root bark of *Cudrania tricuspidata* and their potential neuroprotective effects. *J. Nat. Prod.* 79, 1938–1951.
- Kwon, S.B., Kim, M.J., Yang, J.M., Lee, H.P., Hong, J.T., Jeong, H.S., Kim, E.S., Yoon, D.Y., 2016b. *Cudrania tricuspidata* stem extract induces apoptosis via the extrinsic pathway in SiHa cervical cancer cells. *PLoS One* 11, e0150235.
- Li, Y.Y., Feng, J., Zhang, X.L., Li, M.Q., Cui, Y.Y., 2016. Effects of *Pinus massoniana* bark extract on the invasion capability of HeLa cells. *J. Funct. Foods* 24, 520–526.
- Li, X., Yao, Z., Jiang, X., Sun, J., Ran, G., Yang, X., Zhao, Y., Yan, Y., Chen, Z., Tian, L., Bai, W., 2018 Dec 22. Bioactive compounds from *Cudrania tricuspidata*: A natural anticancer source. *Crit. Rev. Food Sci. Nutr.* 1–21. <https://doi.org/10.1080/10408398>.
- Lu, Y., Shan, S., Li, H., Shi, J., Zhang, X., Li, Z., 2018. Reversal effects of bound polyphenol from foxtail millet bran on multidrug resistance in human HCT-8/fu colorectal cancer cell. *J. Agric. Food Chem.* 66, 5190–5199.
- Lyseng-Williamson, K.A., Fenton, C., 2005. Docetaxel: a review of its use in metastatic breast cancer. *Drugs* 65, 2513–2531.
- Mehta, H.J., Patel, V., Sadikot, R.T., 2014. Curcumin and lung cancer—a review. *Targeted Oncol.* 9, 295–310.
- Paier, C.R.K., Maranhao, S.S., Carneiro, T.R., Lima, L.M., Rocha, D.D., Santos, R.D.S., Farias, K.M., Moraes-Filho, M.O., Pessoa, C., 2018. Natural products as new anti-mitotic compounds for anticancer drug development. *Clinics (Sao Paulo, Brazil)* 73, e813s.
- Park, G.B., Kim, Y.S., Lee, H.-K., Song, H., Kim, S., Cho, D.-H., Hur, D.Y., 2011. Reactive oxygen species and p38 MAPK regulate Bax translocation and calcium redistribution in salubrinal-induced apoptosis of EBV-transformed B cells. *Cancer Lett.* 313, 235–248.
- Radogna, F., Dicato, M., Diederich, M., 2015. Cancer-type-specific crosstalk between autophagy, necroptosis and apoptosis as a pharmacological target. *Biochem. Pharmacol.* 94, 1–11.
- Rakha, E.A., van Deurzen, C.H.M., Paish, E.C., Macmillan, R.D., Ellis, I.O., Lee, A.H.S., 2012. Pleomorphic lobular carcinoma of the breast: is it a prognostically significant pathological subtype independent of histological grade? *Mod. Pathol.* 26, 496.
- Ravindran, J., Gupta, N., Agrawal, M., Bala Bhaskar, A.S., Lakshmana Rao, P.V., 2011. Modulation of ROS/MAPK signaling pathways by kaokaic acid leads to cell death via mitochondrial mediated caspase-dependent mechanism. *Apoptosis* 16, 145–161.
- Siegel, R.L., Miller, K.D., Jemal, A., 2016. Cancer statistics, 2016. *CA: A Clin. J. Clin. Oncol.* 66, 7–30.
- Sui, X., Kong, N., Ye, L., Han, W., Zhou, J., Zhang, Q., He, C., Pan, H., 2014. p38 and JNK

- MAPK pathways control the balance of apoptosis and autophagy in response to chemotherapeutic agents. *Cancer Lett.* 344, 174–179.
- Teixeira, L.L., Costa, G.R., Dorr, F.A., Ong, T.P., Pinto, E., Lajolo, F.M., Hassimotto, N.M.A., 2017. Potential antiproliferative activity of polyphenol metabolites against human breast cancer cells and their urine excretion pattern in healthy subjects following acute intake of a polyphenol-rich juice of grumixama (*Eugenia brasiliensis* Lam.). *Food. Funct.* 8, 2266–2274.
- Tewari, D., Rawat, P., Singh, P.K., 2019. Adverse drug reactions of anticancer drugs derived from natural sources. *Food Chem. Toxicol.: Int. J. Publ. Br. Ind. Biol. Res. Assoc.* 123, 522–535.
- Tian, Y.H., Kim, H.C., Cui, J.M., Kim, Y.C., 2005. Hepatoprotective constituents of *Cudrania tricuspidata*. *Arch. Pharm. Res.* 28, 44–48.
- Vadde, R., Radhakrishnan, S., Kurundu, H.E.K., Reddivari, L., Vanamala, J.K.P., 2016. Indian gooseberry (*Emblica officinalis* Gaertn.) suppresses cell proliferation and induces apoptosis in human colon cancer stem cells independent of p53 status via suppression of c-Myc and cyclin D1. *J. Funct. Foods* 25, 267–278.
- Wilsher, N.E., Arroo, R.R., Matsoukas, M.T., Tsatsakis, A.M., Spandidos, D.A., Androutsopoulos, V.P., 2017. Cytochrome P450 CYP1 metabolism of hydroxylated flavones and flavonols: selective bioactivation of luteolin in breast cancer cells. *Food Chem. Toxicol.* 110, 383–394.
- Woods, D.B., Vousden, K.H., 2001. Regulation of p53 function. *Exp. Cell Res.* 264, 56–66.
- Xin, L.-T., Yue, S.-J., Fan, Y.-C., Wu, J.-S., Yan, D., Guan, H.-S., Wang, C.-Y., 2017. *Cudrania tricuspidata*: an updated review on ethnomedicine, phytochemistry and pharmacology. *RSC Adv.* 7, 31807–31832.
- You, Y., Min, S., Lee, Y.H., Hwang, K., Jun, W., 2017. Hepatoprotective effect of 10% ethanolic extract from *Cudrania tricuspidata* leaves against ethanol-induced oxidative stress through suppression of CYP2E1. *Food Chem. Toxicol.: Int. J. Publ. Br. Ind. Biol. Res. Assoc.* 108, 298–304.
- Zafar, A., Singh, S., Naseem, I., 2017. Cytotoxic activity of soy phytoestrogen coumestrol against human breast cancer MCF-7 cells: insights into the molecular mechanism. *Food Chem. Toxicol.* 99, 149–161.
- Zhang, P., He, D., Chen, Z., Pan, Q., Du, F., Zang, X., Wang, Y., Tang, C., Li, H., Lu, H., Yao, X., Jin, J., Ma, X., 2016. Chemotherapy enhances tumor vascularization via Notch signaling-mediated formation of tumor-derived endothelium in breast cancer. *Biochem. Pharmacol.* 118, 18–30.
- Zhang, Y., Chen, S.G., Wei, C.Y., Rankin, G.O., Rojanasakul, Y., Ren, N., Ye, X.Q., Chen, Y.C., 2018. Dietary compound proanthocyanidins from Chinese bayberry (*Myrica rubra* Sieb. et Zucc.) leaves inhibit angiogenesis and regulate cell cycle of cisplatin-resistant ovarian cancer cells via targeting Akt pathway. *J. Funct. Foods* 40, 573–581.
- Zhao, J., Lu, Y., Shen, H.-M., 2012. Targeting p53 as a therapeutic strategy in sensitizing TRAIL-induced apoptosis in cancer cells. *Cancer Lett.* 314, 8–23.
- Zheng, Z., Zhu, W., Yang, B., Chai, R., Liu, T., Li, F., Ren, G., Ji, S., Liu, S., Li, G., 2018. The co-treatment of metformin with flavone synergistically induces apoptosis through inhibition of PI3K/AKT pathway in breast cancer cells. *Oncol. Lett.* 15, 5952–5958.